Charge Density Wave Melting in One-Dimensional Wires with Femtosecond Subgap Excitation

M. Chávez-Cervantes,* G. E. Topp, S. Aeschlimann, R. Krause, S. A. Sato, M. A. Sentef, and I. Gierz†
Max Planck Institute for the Structure and Dynamics of Matter, Center for Free Electron Laser Science, Hamburg 22761, Germany

(Received 23 October 2018; revised manuscript received 16 May 2019; published 19 July 2019)

Charge density waves (CDWs) are symmetry-broken ground states that commonly occur in low-dimensional metals due to strong electron-electron and/or electron-phonon coupling. The nonequilibrium carrier distribution established via photodoping with femtosecond laser pulses readily quenches these ground states and induces an ultrafast insulator-to-metal phase transition. To date, CDW melting has been mainly investigated in the single-photon regime with pump photon energies bigger than the gap size. The recent development of strong-field midinfrared sources now enables the investigation of CDW dynamics following subgap excitation. Here we excite prototypical one-dimensional indium wires with a CDW gap of ∼300 meV with midinfrared pulses at $\hbar\omega = 190$ meV with MV/cm field strength and probe the transient electronic structure with time- and angle-resolved photoemission spectroscopy. We find that the CDW gap is filled on a timescale short compared to our temporal resolution of 300 fs and that the band structure changes are completed within ∼1 ps. Supported by a minimal theoretical model we attribute our findings to multiphoton absorption across the CDW gap.

DOI: 10.1103/PhysRevLett.123.036405

Large parallel sections on the Fermi surface of one-dimensional metals turn these systems unstable with respect to the formation of charge density waves (CDWs), where strong electron-electron and/or electron-phonon coupling gaps the electronic structure at the Fermi level, resulting in a metal-to-insulator transition below a critical temperature T_C. These CDWs and similar symmetry-broken ground states are readily destroyed via photodoping with femtosecond laser pulses [1–4] as photoexcitation reshapes the potential energy surface of the system and quenches the minimum associated with the symmetry-broken ground state. The corresponding band structure changes are typically traced with femtosecond time- and angle-resolved photoemission spectroscopy (tr-ARPES) as a function of momentum, energy, and time [5–12]. Commonly investigated material systems include Mott insulators, excitonic insulators, Peierls systems, and high-temperature superconductors. The measured melting timescales shed light on the underlying mechanism responsible for the formation of the symmetry-broken ground state [13]. Aside from these fundamental aspects, light-induced insulator-to-metal phase transitions show great potential for future optoelectronic devices such as ultrafast switches or photodetectors.

Depending on photon energy, field strength, and size of the band gap, photodoping—that typically triggers light-induced phase transitions—can occur via single-photon absorption, multiphoton absorption, or tunneling ionization [14]. To date, CDW melting has been mainly investigated in the single-photon regime using pulses with photon energies of ≥1 eV [15–18] and in the tunneling regime with strong-field terahertz (THz) pulses [19–22].

The recent development of midinfrared (MIR) sources with MV/cm field strength [23,24] now enables us to investigate CDW dynamics in the intermediate multiphoton regime. For this purpose we excite prototypical quasi-one-dimensional indium wires that exhibit a CDW gap of ∼300 meV at low temperatures with femtosecond pulses at 190 meV photon energy and use tr-ARPES to record snapshots of the transient electronic structure. We find that the CDW gap is filled on a timescale short compared to our temporal resolution of 300 fs indicating an ultrafast light-induced insulator-to-metal phase transition. The band structure changes are found to be complete after ∼1 ps. We attribute our findings to CDW melting following multiphoton absorption across the CDW gap in good agreement with the observed intensity dependence of the absorbed energy calculated with a minimal model.

Indium atoms deposited on the (7×7) reconstruction of the (111) surface of silicon self-assemble into quasi-one-dimensional chains upon annealing at 400 °C forming a (4×1) surface reconstruction. At room temperature the indium atoms form pairs of zigzag chains [see inset of Fig. 1(b)] separated by one chain of silicon atoms [25]. The band structure has three metallic bands that cross the Fermi level at 0.41 (m_3), 0.54 (m_2), and 0.75 Å^{-1} (m_1) corresponding to band fillings of 0.11 (m_1), 0.38 (m_2), and 0.5 (m_3) [26,27]. Figures 1(a) and 1(b) show the measured Fermi surface and band dispersion along the $\Gamma X \Gamma$ direction of the (4×1) Brillouin zone, respectively. Because of

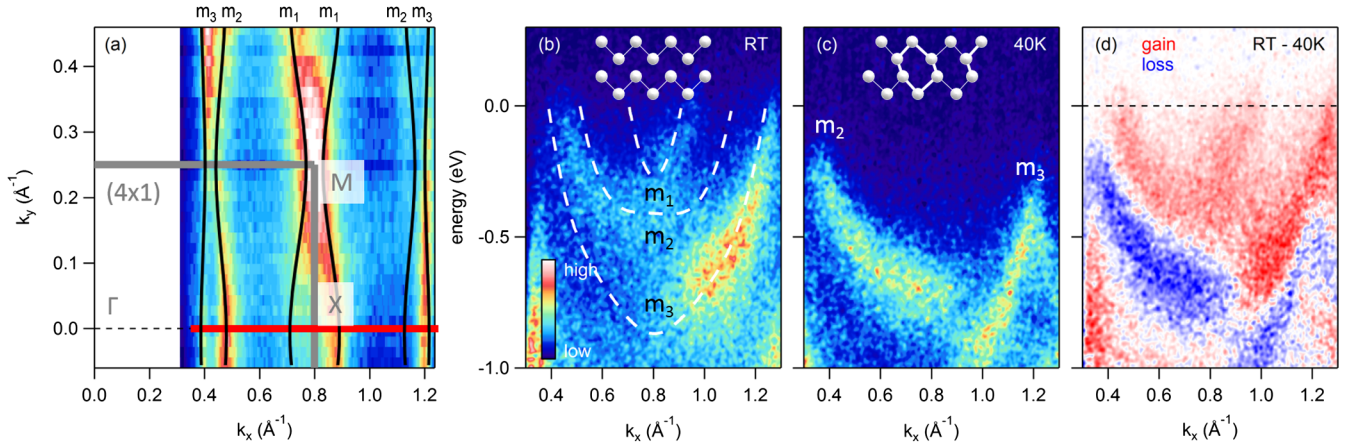

FIG. 1. Equilibrium phase transition. Measured room temperature Fermi surface together with guides to the eye (black), a sketch of the (4×1) Brillouin zone (gray), and a red line indicating the direction along which the dispersion in (b) and (c) is measured. Measured band structure at room temperature (b) and at $T = 40$ K (c). (d) Difference between panel (c) and (b). Insets in (b) and (c) show the respective structure of the Indium wires. White lines in (b) are guides to the eye based on Ref. [31] that mark the position of the bands.

photoemission matrix elements only one half of each band is visible [28].

Below a critical temperature of ~125 K the system undergoes a metal-to-insulator transition into a CDW ground state [27,29,30] with a band gap of ~300 meV [31–33]. A shear distortion that displaces the two zigzag chains in opposite directions parallel to the wires transfers charge from m_1 into m_2. As a result both m_2 and m_3 are half-filled and susceptible to a double-band Peierls transition that is brought about by a dimerization of the outer indium atoms [34,35]. The resulting structure is that of distorted indium hexagons [36] shown in the inset of Fig. 1(c) yielding an (8×2) surface reconstruction. The photoemission spectrum of the insulating phase is shown in Fig. 1(c).

In Fig. 1(d) we show the changes of the photoemission current associated with the equilibrium insulator-to-metal phase transition. This picture was obtained by subtracting Fig. 1(c) from Fig. 1(b). Aside from a pronounced gain just below the Fermi level due to the closing of the band gap, we observe a loss at the position of the low-temperature dispersion, a u-shaped gain at $k_{||} < 1.0$ Å^{-1} close to the Fermi level originating from the charge transfer between m_1 and m_2, and another gain at higher momenta and larger binding energy due to the shift of m_3.

A detailed description of the experimental tr-ARPES setup and the sample preparation is given in the Supplemental Material [37].

In Fig. 2 we present tr-ARPES data taken at a base temperature of 40 K for various pump-probe delays after photoexcitation with 300 fs laser pulses with a photon energy of $\hbar\omega = 190$ meV and a peak electric field of 0.9 MV/cm [37]. Panel (a) shows the temporal average of different tr-ARPES snapshots taken at negative pump-probe delay before the arrival of the pump pulse in the time interval from $t = -700$ to $t = -270$ fs. These data look slightly different from the equilibrium data presented in Fig. 1(c) due to the presence of the pump pulse that broadens the spectral features and causes some spectral weight to reappear at the room temperature position of band m_1 below the Fermi level. We would like to stress that the latter is commonly observed in this material system for pump photon energies ≥1 eV [44,45].

Figure 2(b) shows the photocurrent at $t = 0$ ps, where pump and probe pulses overlap. The corresponding difference spectrum obtained by subtracting panel (a) from panel (b) highlights the pump-induced changes of the photocurrent [Fig. 2(c)]. The signal is dominated by the formation of sidebands of the unperturbed band structure due to laser-assisted photoemission (LAPE) [37]. In Fig. 2(d) we present the tr-ARPES snapshot recorded 1 ps after photoexcitation together with the difference spectrum in Fig. 2(e). The observed gain and loss features closely resemble those for the equilibrium insulator-to-metal transition in Fig. 1(d), suggesting a transient melting of the CDW.

For a quantitative analysis of the CDW melting we integrate the pump-induced changes of the photocurrent in different areas marked by black boxes in Fig. 2(e) that highlight three main features associated with CDW melting: the in-gap spectral weight (box 1), the shift of m_1 below the Fermi level (box 2), and the shift of m_3 towards the Fermi level (box 3). The integrated photocurrent is presented in Fig. 3 as a function of pump-probe delay for three different field strengths. For field strengths of 0.3 and 0.7 MV/cm all boxes exhibit a short-lived pump-probe signal that only exists in the presence of the pump pulse indicative of LAPE [37]. For a field strength of 0.9 MV/cm the pump-probe signal persists after the pulse is gone. In this case, the rise time of the in-gap spectral weight in Fig. 3(a) is found to be shorter than the pulse duration of 300 fs. From error-function fits of the rising edge of the

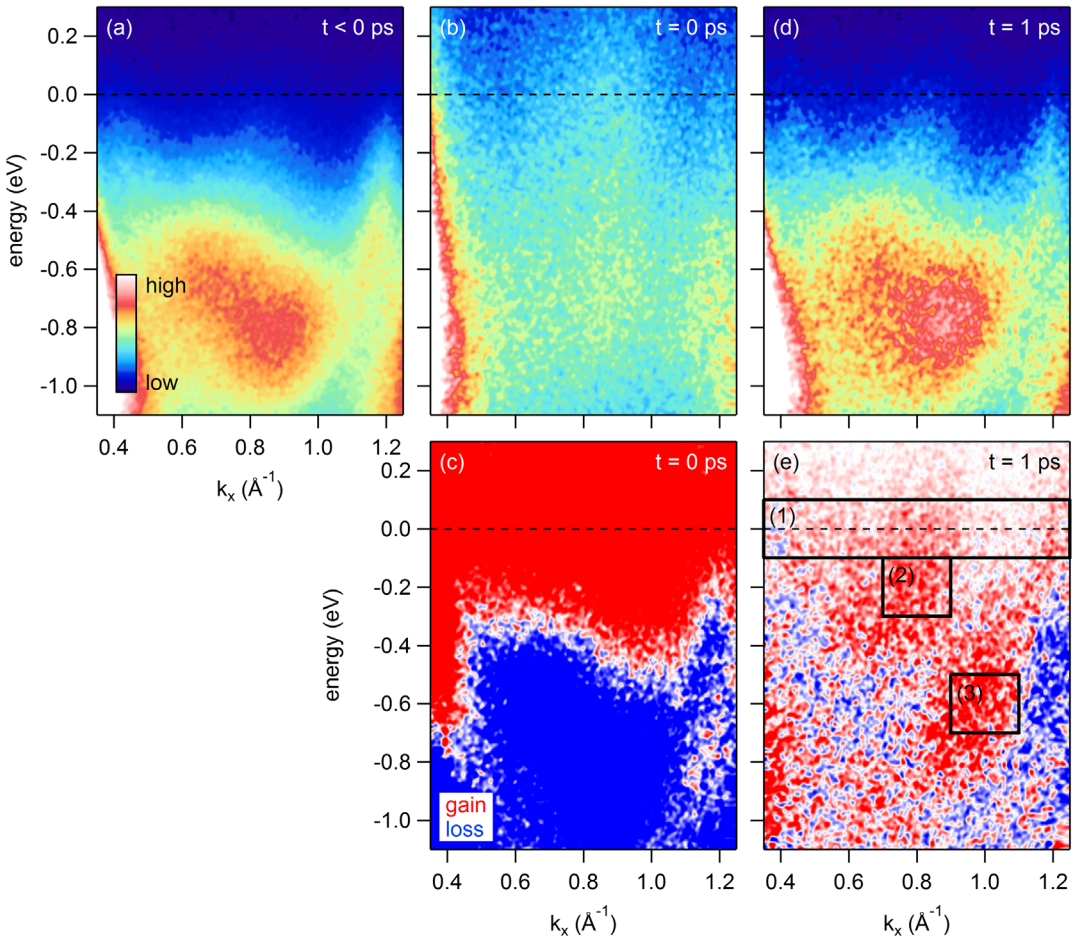

FIG. 2. Light-induced phase transition. (a) Measured band structure at negative pump-probe delay. (b) Measured photocurrent in the presence of the 300 fs pump pulse at $\hbar\omega = 190$ meV with a peak electric field of 0.9 MV/cm. (c) Same as (b) but for a pump-probe delay of 1 ps. (d),(e) The pump-induced changes of the photocurrent obtained by subtracting panel (a) from panels (b) and (c), respectively. Black boxes in (e) indicate the area over which the pump-probe signal in Fig. 3 was integrated.

pump-probe signal [37] in Figs. 3(b) and 3(c) we find that the band structure changes occur within ~1 ps. The lifetime of the transient metallic state is found to be 6 ± 1 ps from exponential fits of the decay of the spectral weight shown in Fig. 3(d).

After providing direct experimental evidence for CDW melting in one-dimensional indium wires with strong pump pulses, the photon energy of which is smaller than the CDW gap in Figs. 2 and 3, we now set out to unravel the underlying mechanism. For this purpose we compare the observed timescales with previous time-resolved electron diffraction (tr-RHEED) [18,46] and tr-ARPES investigations [44,45] for photoexcitation at $\hbar\omega \geq 1$ eV. There, the band gap in m_2 and m_3 was found to close within 200 fs [45], and the structural (8×2) to (4×1) transition was found to be complete within ~700 fs [44–46]. Our rise times are very similar which indicates that the same microscopic mechanism that is described in detail below is at work. Further, Ref. [46] found that the timescale for the structural phase transition decreased with increasing fluence. Also, for excitation densities below 0.4 electrons per (8×2) unit cell, the structural phase transition was found to remain incomplete [46], which is expected to reduce the lifetime of the transient metallic state considerably [18]. The fact that the rise times in the present study are slightly longer and the lifetime of the metallic state is significantly shorter compared to previous studies [18,44–46] indicates that CDW melting in the present case might be incomplete.

Based on density functional theory and *ab initio* molecular dynamics simulations the following microscopic understanding of the light-induced phase transition in In/Si(111) has emerged [45,46]: Holes generated at the (8×2) zone boundary were shown to break the In-In dimer bonds between the outer In chain atoms and thereby lift the dimerization that gaps m_2 and m_3. Electrons that transiently occupy the conduction band close to the (8×2) zone center were shown to form bonds across neighboring In zigzag chains, thereby lifting the shear distortion and shifting m_1 below the Fermi level. The experimentally observed

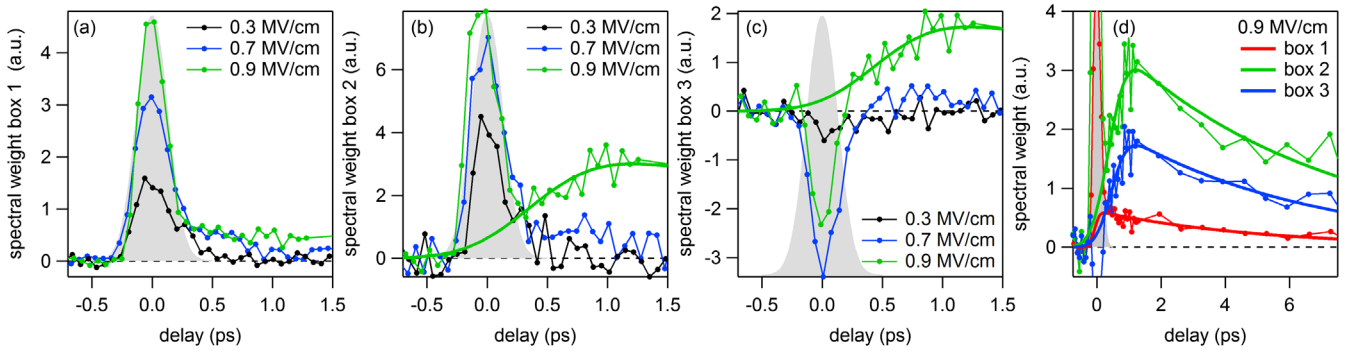

FIG. 3. CDW melting dynamics. Pump-probe signal obtained by integrating the pump-induced changes of the photocurrent over the areas marked by the black boxes in Fig. 2(e). The gray-shaded region is the pump pulse. (a) In-gap spectral weight as a function of pump-probe delay for different peak field strengths from box (1). (b) Downshift of m_1 from box (2) with a rise time of 1.0 ± 0.2 ps. (c) Upshift of m_3 from box (3) with a rise time of 0.9 ± 0.2 ps [37]. (d) Long-time dynamics of the spectral weight in boxes 1–3 yielding exponential life times of 6 ± 1 ps. Thick lines in (b)–(d) are fits to the data [37].

timescales roughly correspond to one-quarter of the period of the rotary and shear phonon modes [46] consistent with a Peierls transition.

Aside from single-photon absorption, multiphoton absorption and tunneling ionization emerge as alternative scenarios that might provide the nonequilibrium carrier distribution required to drive the insulator-to-metal phase transition in the indium wires used in the present study. Tunneling ionization and multiphoton absorption can be easily distinguished by considering the Keldysh parameter γ that is given by the square root of the ratio between gap size and ponderomotive energy [14]. $\gamma > 1$ and $\gamma < 1$ correspond to photoexcitation via multiphoton absorption and tunneling ionization, respectively [14]. From the experimental parameters we obtain $\gamma_{\mathrm{exp}} = 1.6$ [37] implying multiphoton absorption.

In order to support this interpretation, we simulate the interaction of the MIR pump pulse with our sample [37] and calculate the change in total energy of the system ΔE for different field strengths as a function of pump-probe delay shown in Fig. 4(a). We find that for field strengths above ~1 MV/cm the absorbed energy (ΔE at $t = 500$ fs after the pulse is gone) exceeds the CDW condensation energy of 32 meV at $T = 40$ K [47] and the CDW is expected to melt. The theoretically predicted threshold field agrees well with the experimental value of ~0.9 MV/cm [37].

The log-log plot of absorbed energy vs intensity (field squared) in Fig. 4(b) allows us to distinguish between the multiphoton and the tunneling regime as the two regimes exhibit different slopes. For fields below 1.3 MV/cm we fit a slope of two indicating that each photoexcited electron absorbs two photons. For higher fields the absorbed energy exhibits a slower increase indicating tunneling ionization. Note that the deviation from the quadratic intensity dependence coincides with the crossover between $\gamma > 1$ and $\gamma < 1$ [blue-shaded area in Fig. 4(b)] and that the threshold field for CDW melting lies in the multiphoton

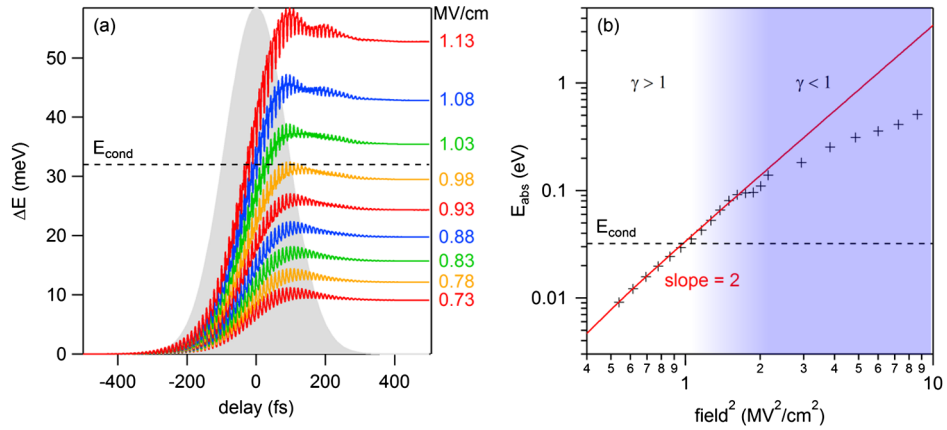

FIG. 4. Simulation. (a) Change in total energy ΔE of the system as a function of time for different peak field strengths. The dashed line indicates the CDW condensation energy of 32 meV per (4×2) unit cell [37]. The gray-shaded area is the pump pulse. (b) Log-log plot of absorbed energy vs the square of the peak field. The red line has a slope of 2 as expected for two-photon absorption. White and blue areas distinguish the multiphoton ($\gamma > 1$) and the tunneling regime ($\gamma < 1$), respectively.

regime in agreement with the experimental Keldysh parameter.

Before establishing multiphoton absorption as the main reason for CDW melting in the present study, we need to exclude several alternative scenarios that have been previously evoked to explain related insulator-to-metal phase transitions following photoexcitation with strong MIR and THz pulses.

Reference [48] showed that MIR pulses at $\hbar\omega = 400$ meV, resonant to an optical transition between the backfolded valence and conduction band, melts the CDW in 1T-$TiSe_2$. Our pump photon energy is significantly smaller than the gap size which is why we exclude single-photon absorption across the gap as a possible route for CDW melting in the present case. Also, the employed pump photon energy is much smaller than the indirect band gap of silicon, $E_{\mathrm{gap}} = 1.1$ eV. Therefore, substrate-induced effects such as a transient heating of the sample above the critical temperature are unlikely [49].

Further, Ref. [50] showed that resonant excitation of an infrared-active phonon mode at $\hbar\omega = 71$ meV results in a 5 orders of magnitude drop in resistivity in $Pr_{0.7}Ca_{0.3}MnO_3$. The In/Si(111)-(8×2) phase has maximum phonon frequencies on the order of a few THz (a few tens of meV) [51,52] much smaller than the pump photon energy of 190 meV such that we can also exclude a resonant excitation of the lattice.

Alternatively, Ref. [19] demonstrated that defect-mediated subgap absorption at $\hbar\omega = 180$ meV $< E_{\mathrm{gap}} =$ 670 meV in polycrystalline VO_2 films is strong enough to drive the insulator-to-metal phase transition. Because of the single-crystalline nature of our samples [37] we consider defect-mediated subgap absorption too weak to be able to drive the insulator-to-metal phase transition in the present study.

Finally, we already excluded tunneling ionization that was evoked to explain the THz-driven insulator-to-metal phase transition in VO_2 single crystals [21,22].

Therefore, the only scenario that seems to be able to account for the observed CDW melting in the present study is multiphoton absorption.

In summary, we have used tr-ARPES to probe the band structure changes induced by strong-field MIR excitation at photon energies smaller than the CDW gap in quasi-one-dimensional indium wires. We observe a transient melting of the CDW on a timescale that is similar to the one observed at pump photon energies $\hbar\omega \geq 1$ eV, indicating a similar microscopic melting mechanism. We attribute our results to photodoping via multiphoton absorption based on the excellent quantitative agreement between our data and a minimal theoretical model. Our findings are relevant for ultrafast optical switching and open new pathways for MIR detection.

We thank A. Rubio for many helpful discussions and acknowledge financial support from the German Science Foundation through the Collaborative Research Center CRC925 and the Emmy Noether program (SE 2558/2-1).

*mariana.chavez-cervantes@mpsd.mpg.de
†isabella.gierz@mpsd.mpg.de

[1] A. Cavalleri, C. Tóth, C. W. Siders, J. A. Squier, F. Ráksi, P. Forget, and J. C. Kieffer, Phys. Rev. Lett. **87**, 237401 (2001).
[2] S. Iwai, M. Ono, A. Maeda, H. Matsuzaki, H. Kishida, H. Okamoto, and Y. Tokura, Phys. Rev. Lett. **91**, 057401 (2003).
[3] M. Chollet, L. Guerin, N. Uchida, S. Fukaya, H. Shimoda, T. Ishikawa, K. Matsuda, T. Hasegawa, A. Ota, H. Yamochi, G. Saito, R. Tazaki, S. Adachi, and S. Koshihara, Science **307**, 86 (2005).
[4] P. Kusar, V. V. Kabanov, J. Demsar, T. Mertelj, S. Sugai, and D. Mihailovic, Phys. Rev. Lett. **101**, 227001 (2008).
[5] L. Perfetti, P. A. Loukakos, M. Lisowski, U. Bovensiepen, H. Berger, S. Biermann, P. S. Cornaglia, A. Georges, and M. Wolf, Phys. Rev. Lett. **97**, 067402 (2006).
[6] F. Schmitt, P. S. Kirchmann, U. Bovensiepen, R. G. Moore, L. Rettig, M. Krenz, J.-H. Chu, N. Ru, L. Perfetti, D. H. Lu, M. Wolf, I. R. Fisher, and Z.-X. Shen, Science **321**, 1649 (2008).
[7] T. Rohwer, S. Hellmann, M. Wiesenmayer, C. Sohrt, A. Stange, B. Slomski, A. Carr, Y. Liu, L. M. Avila, M. Kalläne, S. Mathias, L. Kipp, K. Rossnagel, and M. Bauer, Nature (London) **471**, 490 (2011).
[8] J. C. Petersen, S. Kaiser, N. Dean, A. Simoncig, H. Y. Liu, A. L. Cavalieri, C. Cacho, I. C. E. Turcu, E. Springate, F. Frassetto, L. Poletto, S. S. Dhesi, H. Berger, and A. Cavalleri, Phys. Rev. Lett. **107**, 177402 (2011).
[9] S. Hellmann, T. Rohwer, M. Kalläne, K. Hanff, C. Sohrt, A. Stange, A. Carr, M. M. Murnane, H. C. Kapteyn, L. Kipp, M. Bauer, and K. Rossnagel, Nat. Commun. **3**, 1069 (2012).
[10] H. Y. Liu, I. Gierz, J. C. Petersen, S. Kaiser, A. Simoncig, A. L. Cavalieri, C. Cacho, I. C. E. Turcu, E. Springate, F. Frassetto, L. Poletto, S. S. Dhesi, Z.-A. Xu, T. Cuk, R. Merlin, and A. Cavalleri, Phys. Rev. B **88**, 045104 (2013).
[11] S. Mathias *et al.*, Nat. Commun. **7**, 12902 (2016).
[12] L. Rettig, R. Cortés, J.-H. Chu, I. R. Fisher, F. Schmitt, R. G. Moore, Z.-X. Shen, P. S. Kirchmann, M. Wolf, and U. Bovensiepen, Nat. Commun. **7**, 10459 (2016).
[13] C. Sohrt, A. Stange, M. Bauer, and K. Rossnagel, Faraday Discuss. **171**, 243 (2014).
[14] L. Keldysh, Zh. Eksp. Teor. Fiz. **47**, 1945 (1965).[Sov. Phys. JETP **20**, 1307 (1965)].
[15] A. Cavalleri, T. Dekorsy, H. H. W. Chong, J. C. Kieffer, and R. W. Schoenlein, Phys. Rev. B **70**, 161102(R) (2004).
[16] A. Tomeljak, H. Schäfer, D. Städter, M. Beyer, K. Biljakovic, and J. Demsar, Phys. Rev. Lett. **102**, 066404 (2009).
[17] S. Hellmann, M. Beye, C. Sohrt, T. Rohwer, F. Sorgenfrei, H. Redlin, M. Kalläne, M. Marczynski-Bühlow, F. Hennies, M. Bauer, A. Föhlisch, L. Kipp, W. Wurth, and K. Rossnagel, Phys. Rev. Lett. **105**, 187401 (2010).
[18] S. Wall, B. Krenzer, S. Wippermann, S. Sanna, F. Klasing, A. Hanisch-Blicharski, M. Kammler, W. G. Schmidt, and M. Horn-von Hoegen, Phys. Rev. Lett. **109**, 186101 (2012).

[19] M. Rini, Z. Hao, R. W. Schoenlein, C. Giannetti, F. Parmigiani, S. Fourmaux, A. Fujimori, M. Onoda, S. Wall, and A. Cavalleri, Appl. Phys. Lett. **92**, 181904 (2008).
[20] M. Liu, H. Y. Hwang, H. Tao, A. C. Strikwerda, K. Fan, G. R. Keiser, A. J. Sternbach, K. G. West, S. Kittiwatanakul, J. Lu, S. A. Wolf, F. G. Omenetto, X. Zhang, K. A. Nelson, and R. D. Averitt, Nature (London) **487**, 345 (2012).
[21] B. Mayer, C. Schmidt, A. Grupp, J. Bühler, J. Oelmann, R. E. Marvel, R. F. Haglund, Jr., T. Oka, D. Brida, A. Leitenstorfer, and A. Pashkin, Phys. Rev. B **91**, 235113 (2015).
[22] A. X. Gray *et al.*, Phys. Rev. B **98**, 045104 (2018).
[23] R. A. Kaindl, M. Wurm, K. Reinmann, P. Hamm, A. H. Weiner, and M. Woerner, J. Opt. Soc. Am. B **17**, 2086 (2000).
[24] C. Ventalon, J. M. Fraser, J. P. Likforman, D. M. Villeneuve, P. B. Corkum, and M. Joffre, J. Opt. Soc. Am. B **23**, 332 (2006).
[25] O. Bunk, G. Falkenberg, J. H. Zeysing, L. Lottermoser, R. L. Johnson, M. Nielsen, F. Berg-Rasmussen, J. Baker, and R. Feidenhans'l, Phys. Rev. B **59**, 12228 (1999).
[26] T. Abukawa, M. Sasaki, F. Hisamatsu, T. Goto, T. Kinoshita, A. Kakizaki, and S. Kono, Surf. Sci. **325**, 33 (1995).
[27] J. R. Ahn, J. H. Byun, H. Koh, E. Rotenberg, S. D. Kevan, and H. W. Yeom, Phys. Rev. Lett. **93**, 106401 (2004).
[28] H. Morikawa, C. C. Hwang, and H. W. Yeom, Phys. Rev. B **81**, 075401 (2010).
[29] H. W. Yeom, S. Takeda, E. Rotenberg, I. Matsuda, K. Horikoshi, J. Schaefer, C. M. Lee, S. D. Kevan, T. Ohta, T. Nagao, and S. Hasegawa, Phys. Rev. Lett. **82**, 4898 (1999).
[30] Y. J. Sun, S. Agario, S. Souma, K. Sugawara, Y. Tago, T. Sato, and T. Takahashi, Phys. Rev. B **77**, 125115 (2008).
[31] S.-W. Kim and J.-H. Cho, Phys. Rev. B **93**, 241408(R) (2016).
[32] S. Chandola, K. Hinrichs, M. Gensch, N. Esser, S. Wippermann, W. G. Schmidt, F. Bechstedt, K. Fleischer, and J. F. McGlip, Phys. Rev. Lett. **102**, 226805 (2009).
[33] T. Tanikawa, I. Matsuda, T. Kanagawa, and S. Hasegawa, Phys. Rev. Lett. **93**, 016801 (2004).
[34] C. González, J. Ortega, and F. Flores, New J. Phys. **7**, 100 (2005).
[35] E. Jeckelmann, S. Sanna, W. G. Schmidt, E. Speiser, and N. Esser, Phys. Rev. B **93**, 241407(R) (2016).
[36] C. Kumpf, O. Bunk, J. H. Zeysing, Y. Su, M. Nielsen, R. L. Johnson, R. Feidenhans'l, and K. Bechgaard, Phys. Rev. Lett. **85**, 4916 (2000).
[37] See Supplemental Material at http://link.aps.org/supplemental/10.1103/PhysRevLett.123.036405 for further information about sample growth, tr-ARPES setup, data analysis, and model including Refs. [38–43].
[38] J. L. Stevens, M. S. Worthington, and I. S. T. Tsong, Phys. Rev. B **47**, 1453 (1993).
[39] J.-L. Lin, D. Y. Petrovykh, J. Viernow, F. K. Men, D. J. Seo, and F. J. Himpsel, J. Appl. Phys. **84**, 255 (1998).
[40] F. Frassetto, C. Cacho, C. A. Froud, I. C. E. Turcu, P. Villoresi, W. A. Bryan, E. Springate, and L. Poletto, Opt. Express **19**, 19169 (2011).
[41] G. Saathoff, L. Miaja-Avila, M. Aeschlimann, M. M. Murnane, and H. C. Kapteyn, Phys. Rev. A **77**, 022903 (2008).
[42] M. A. Sentef, M. Claassen, A. F. Kemper, B. Moritz, T. Oka, J. K. Freericks, and T. Devereaux, Nat. Commun. **6**, 7047 (2015).
[43] H. W. Yeom, K. Horikoshi, H. M. Zhang, K. Ono, and R. I. G. Uhrberg, Phys. Rev. B **65**, 241307 (2002).
[44] M. Chavez-Cervantes, R. Krause, S. Aeschlimann, and I. Gierz, Phys. Rev. B **97**, 201401(R) (2018).
[45] C. W. Nicholson, A. Lücke, W. G. Schmidt, M. Puppin, L. Rettig, R. Ernstorfer, and M. Wolf, Science **362**, 821 (2018).
[46] T. Frigge, B. Hafke, T. Witte, B. Krenzer, C. Streubühr, A. Samad Syed, V. Mikšić Trontl, I. Avigo, P. Zhou, M. Ligges, D. von der Linde, U. Bovensiepen, M. Horn-von Hoegen, S. Wippermann, A. Lüke, S. Sanna, U. Gerstmann, and W. G. Schmidt, Nature (London) **544**, 207 (2017).
[47] S. Wippermann and W. G. Schmidt, Phys. Rev. Lett. **105**, 126102 (2010).
[48] C. Monney, M. Puppin, C. W. Nicholson, M. Hoesch, R. T. Chapman, E. Springate, H. Berger, A. Magrez, C. Cacho, R. Ernstorfer, and M. Wolf, Phys. Rev. B **94**, 165165 (2016).
[49] C. W. Nicholson, M. Puppin, A. Lücke, U. Gerstmann, M. Krenz, W. G. Schmidt, L. Rettig, R. Ernstorfer, and M. Wolf, Phys. Rev. B **99**, 155107 (2019).
[50] M. Rini, R. Tobey, N. Dean, J. Itatani, Y. Tomioka, Y. Tokura, R. W. Schoenlein, and A. Cavalleri, Nature (London) **449**, 72 (2007).
[51] K. Fleischer, S. Chandola, N. Esser, W. Richter, and J. F. McGilp, Phys. Rev. B **76**, 205406 (2007).
[52] E. Speiser, N. Esser, S. Wippermann, and W. G. Schmidt, Phys. Rev. B **94**, 075417 (2016).